7-1975

Scattering of Ultrasonic Pulses from Cylindrical Inclusions in Elastic Solids

Wolfgang Sachse
Cornell University

Scattering of Ultrasonic Pulses from Cylindrical Inclusions in Elastic Solids

Abstract
I would like to review today the work that we have been doing in the Mechanics Department at Cornell in studying the scattering of ultrasonic pulses by a cylindrical inclusion. A large portion of this work has been supported by the National Science Foundation through a grant to the Materials Science Center at Cornell. This work is the result of a very close interaction between the theoretical studies that have been made by Professor Pao, his students and his associates, and the experimental work that has been done by my students and myself. The first results I will describe have previously been reported in several publications while the later work is taken from the dissertation of Bifulco and a forthcoming publication.

Disciplines
Materials Science and Engineering | Structures and Materials

SCATTERING OF ULTRASONIC PULSES FROM CYLINDRICAL INCLUSIONS IN ELASTIC SOLIDS

Wolfgang Sachse
Cornell University
Ithaca, New York

I would like to review today the work that we have been doing in the Mechanics Department at Cornell in studying the scattering of ultrasonic pulses by a cylindrical inclusion. A large portion of this work has been supported by the National Science Foundation through a grant to the Materials Science Center at Cornell. This work is the result of a very close interaction between the theoretical studies that have been made by Professor Pao, his students and his associates, and the experimental work that has been done by my students and myself. The first results I will describe have previously been reported in several publications[1,2,3] while the later work is taken from the dissertation of Bifulco[4] and a forthcoming publication[5].

We set out initially to see if we could understand in some rational way the pronounced differences that are observed in the power spectra of ultrasonic pulses when they are scattered by various flaws in elastic solids. We hoped that our results would permit us to understand better the physics of elastic wave scattering and also that our results would find some application for the quantitative, nondestructive testing or evaluation of materials.

Our reason for using cylindrical scatterers is two-fold: one, the exact solution of the scattering by such an object has been worked out completely and secondly, the fabrication of specimens containing such scatters is quite easy and quite inexpensive. This entire research program that I'm describing is really a very low-budget program. So, these specimens fit our needs perfectly. We believe, however, that our results are perfectly general and that they can be applied to any other scattering situation in which the scatterer is convex and has no sharp edges.

In this work we have used pulse arrival time and ultrasonic pulse spectroscopy measurements of the scattered signals and we interpreted these in terms of the ray theory of geometric acoustics and the normal mode theory of a resonating inclusion respectively.

Let me first briefly review some of the early work that we have done on the scattering by an isolated fluid-filled inclusion in elastic solid.

In Fig. 1, I show the experimental setup we used in these experiments. It is a standard pulse echo system consisting of a broad-band pulser, attached to a wide-band transducer. The return signals are amplified by a wide-band amplifier and displayed on the display oscilloscope. We photographed this oscilloscope, made enlargements to obtain 8 by 10 in. prints, and then digitized the signals by hand into a PDP-15 computer. There we computed the Fourier amplitudes and the Fourier power spectra. The results were plotted

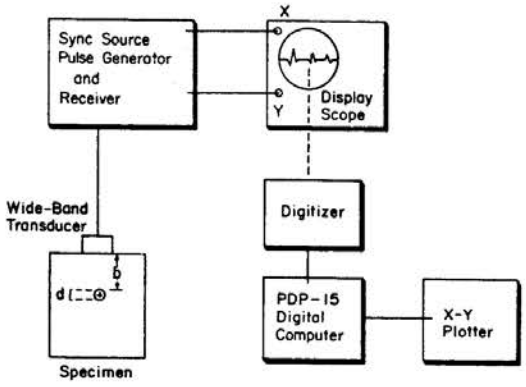

Fig. 1. Schematic of experimental setup.

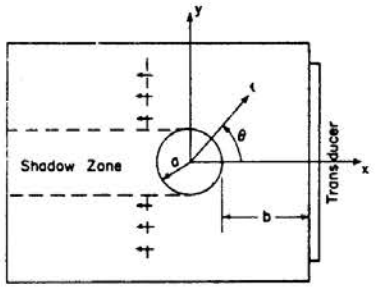

Fig. 2. Geometry of the isolated inclusion specimen and the incident wave.

with an x-y digital plotter. All the spectra that I will show you were obtained in this way. The arrival time measurements we made directly from the oscilloscope using its delaying circuitry or from the photographic enlargements of the oscilloscope traces.

Figure 2 shows a schematic diagram of our specimen setup. On the right is attached the broadband transducer, and our inclusion is a distance of b away from it. The inclusion radius is given by a . We see that if a wave is incident on the inclusion, the forward edge of the inclusion will be illuminated and the backward surface will be in the shadow zone.

We considered inclusions in matrix materials such that we could investigate a broad range of scattering situations. Figure 3 shows the types of materials that we have used. The matrix materials are listed at the top, and the inclusion fluids are at the bottom.

The characteristic amplitude-time record that we observed for the isolated fluid-filled inclusion is shown in Fig. 4. We show the case of a 1/16 in. diameter water-filled inclusion in an aluminum block. The first signal returned from the inclusion we call A_1. It is, of course, the reflection from the forward edge of the inclusion and people have observed this for years. It's arrival-time depends upon the location of the inclusion. The large amplitude which we call B_1 corresponds to a specular reflection from the back side of the specimen. The origin of the other amplitudes we didn't understand at first. We observed that the amplitudes A_2, A_3 depended very critically on what was contained in the inclusion as well as what the size of the inclusion was. Similarly for the small amplitude labelled a_2. However, contrary to that, the amplitude a_1 was very reproducible, and its arrival appeared to be totally independent of what was contained in the inclusion. It depended only on the size of the inclusion.

Once we observed amplitude-time traces like this and they were very reproducible, we tried to understand how do these things arise? And, of course, since we're primarily interested in the arrival-time, it's very natural to consider what are the arrival-times of various acoustic rays which return to the transducer from the inclusion.

Well, it turns out that we could account for the arrival of each of the signals emanating from the inclusion in terms of the motion of four wavefronts. Shown in Fig. 5 are the reflected wavefront from the illuminated side of the inclusion and the diffracted wavefront which travels behind the inclusion. Not shown in the figure are the two refracted wavefronts inside of the inclusion. There is a reflected wavefront from the illuminated side, that is the side facing the transducer and there is a refracted wavefront from the shadow side. The orthonormal trajectories to these wavefronts are called the rays. The four principal rays which are back scattered to the transducer are shown in Fig. 6. The notation we use here is borrowed from seismology. Here P represents a compressional wave propagating in the matrix and F represents a compressional wave propagating in the inclusion fluid.

Table I(a)

PROPERTIES OF MATRIX MATERIALS

	Aluminum	Lucite	Polystyrene	Tin	Lead
Density (g/cm^3)	2.70	1.18	1.06	7.30	11.34
Wave Speed c_p(cm-μsec)	0.638	0.272	0.235	0.332	0.215

TABLE I(b)

PROPERTIES OF INCLUSION FLUIDS

	Air	Water	Carbon Tetra-Chloride	Alcohol	Glycerin
Density (g/cm^3)	1.29×10^{-3}	1.000	1.596	0.792	1.26
Wave Speed c_f(cm/μsec)	0.0332	0.149	0.0929	0.111	0.199

Fig. 3. Table I(a) - Properties of matrix materials.
Table I(b) - Properties of inclusion fluids.

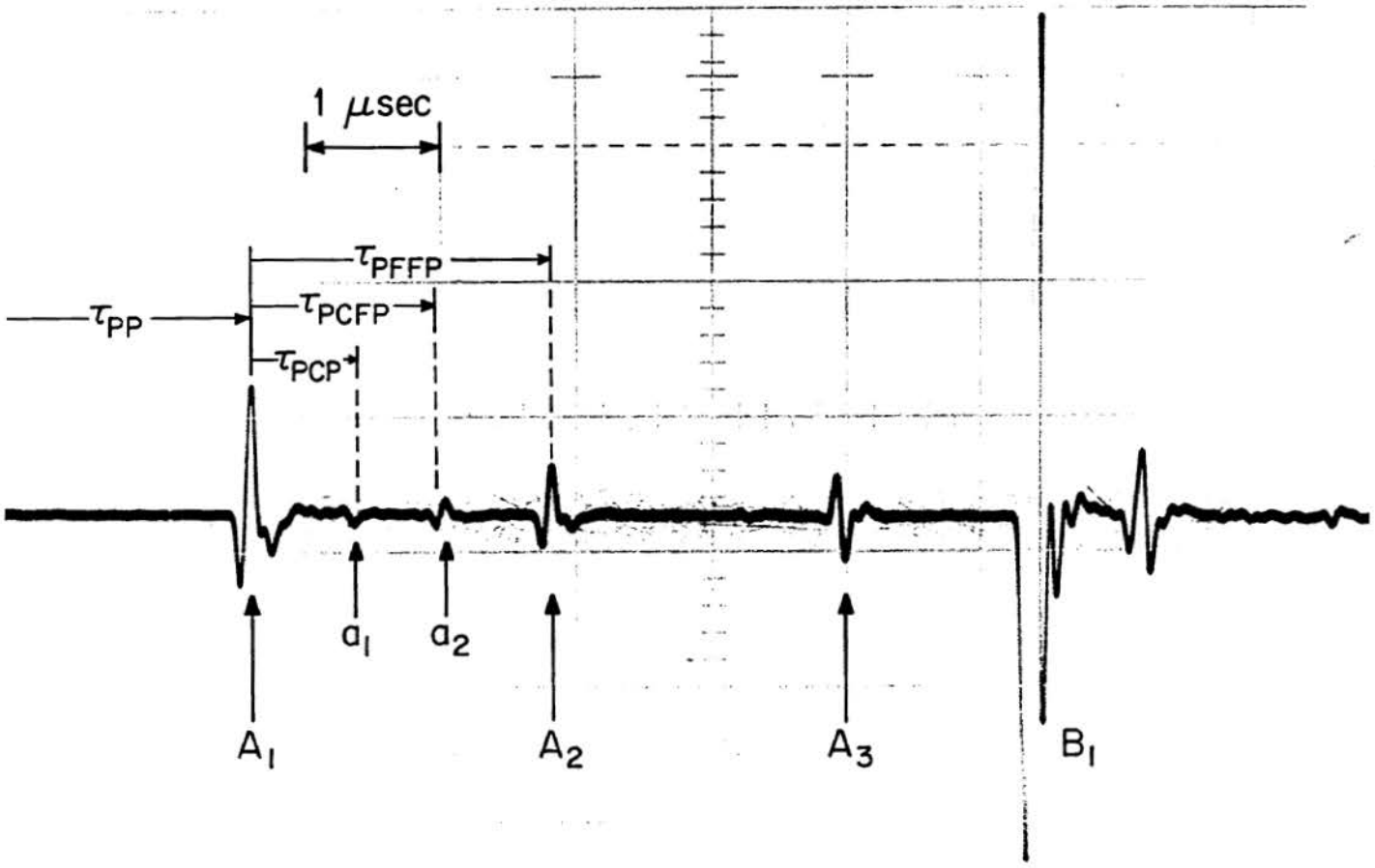

Fig. 4. Typical amplitude-time record. Shown is the case of a 1/16-in. diameter, water-filled inclusion in aluminum.

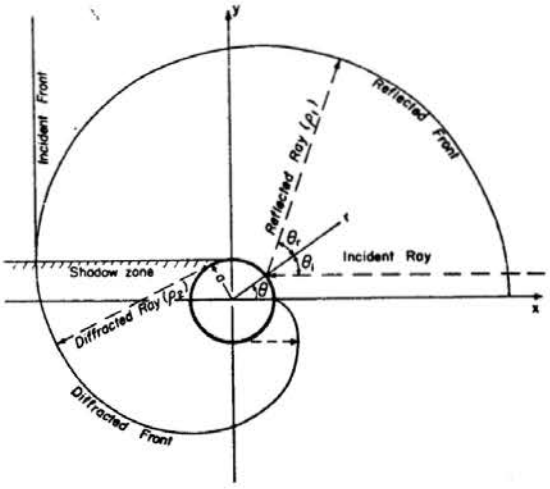

Fig. 5. Reflection and diffraction of waves at a circular inclusion.

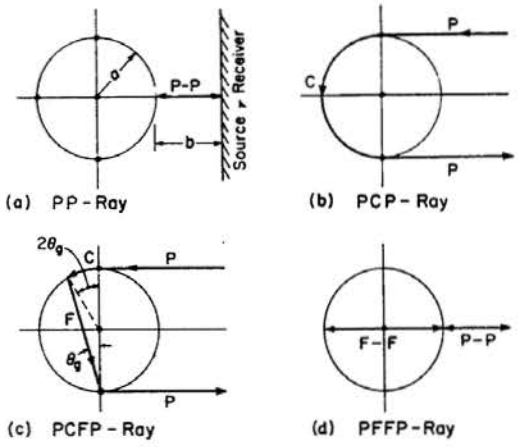

Fig. 6. Four rays emitted and received by the transducer.

The first ray, that is the ray which is associated with the wavefront reflected from the illuminated side of the inclusion, we denote as the P-P ray. The next ray which we immediately identified, is the ray which corresponds to the wavefront incident on the forward edge of the inclusion, propagating through the inclusion and being reflected and returned to the transducer. We've labeled this as the PFFP ray.

The next ray that we identified was the PCP ray. This is the ray which is tangent to the edge of the inclusion and is diffracted around the cylinder back to the transducer. Neubauer[6] has observed the propagation of this ray with a Schlieren technique for the case of a solid cylinder in water.

The other ray is the PCFP ray, and this corresponds to a ray which creeps along the circumference of the inclusion then propagates through the fluid medium and returns to the transducer. We call this ray the "halo" ray because of its similarity to the case in optics. Having found the ray paths, we can easily compute what the arrival times of the associated rays are by simply taking the distance that each ray travels and dividing it by the wave speed of the medium in which it is propagating.

It is thus clear now the various signals shown in Fig. 4 are to be associated with the various rays. The arrival times are labelled τ_{PP}, τ_{PCP}, τ_{PCFP} and τ_{PFFP} in the figure. The comparison between calculated and measured arrival times for inclusions in aluminum, as well as various inclusions in other solid materials shows agreement in all cases to be better than 10%.

We found that the equations for the arrival times depended very strongly on the ratio of the wave speed in the fluid to that of the solid. We call this ratio γ. We, therefore, investigated experimentally whether these equations would still correctly predict the arrival times of the rays from inclusions of various sizes as γ approaches 1.0.

We show in Fig. 7 the results of measurements made on different sizes of inclusions filled with various fluids in aluminum, Lucite and lead. The ordinate axis of the figure is the measured arrival time normalized with respect to the arrival time one expects if the inclusion consisted entirely of matrix material. It is clear that the arrival times of the signals are a function of what is in the inclusion. The solid lines in the figure are the computed arrival times and the points are the measured data. Except for the PCP arrival time data, which is quite difficult to measure because the a_1 amplitude is so small, the agreement between predicted and observed arrival times is quite good over a broad range of matrix inclusion materials.

To see whether we could use our ray arrival-time equations in a quantitative NDE application, we solved them for the quantities which describe the location, size and wave speed as shown in Fig. 8. The equation for b specifies the location of the inclusion. It is the well known equation one uses in determining the location of flaws in materials. It is simply the arrival-time of the A_1 amplitude τ_{PP} divided by c_p, the wave speed in the matrix material. The

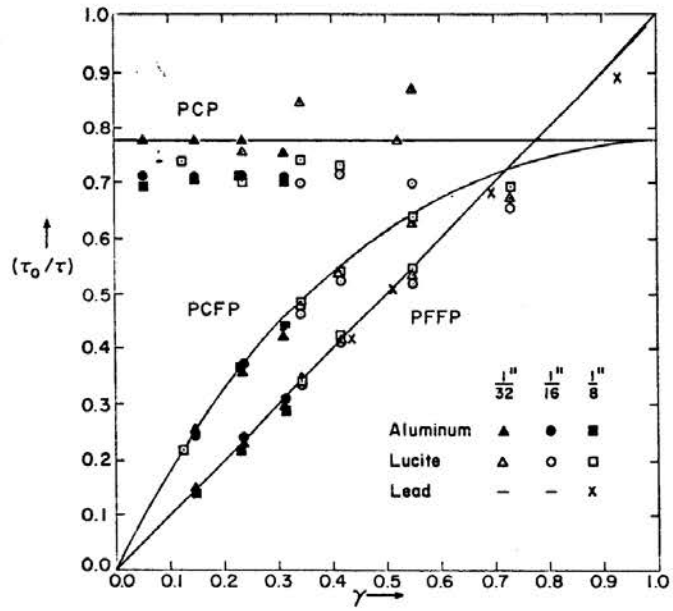

Fig. 7. The computed and measured relative arrival times τ_{PCP}, τ_{PCFP} and τ_{PFFP} as a function of γ, the fluid-to-solid wave-speed ratio.

$$b = \tau_{pp}/c_p$$

$$a = \left[c_p/(2+\pi) \right] \tau_{PCP}$$

$$c_f = 4a/\tau_{PFFP}$$

$$c_f = \left[\frac{4c_p}{(2+\pi)} \right] \frac{\tau_{PCP}}{\tau_{PFFP}}$$

Fig. 8. Equations for the location, radius and fluid wave speed in terms of the ray arrival-times.

equation for the inclusion radius a can be evaluated from measurements of the arrival time of the PCP amplitude (τ_{PCP}).

Finally, the equation for the fluid's wave speed c_f is simply equal to twice the diameter (4a) divided by the arrival time of the A_2 amplitude with respect to amplitude A_1 (τ_{PFFP}). The equations for a and c_f can be combined as shown to find c_f in terms of the measurements of τ_{PCP} and τ_{PFFP} alone. We now have a way of determining the location, the size and what is the inclusion fluid's wave speed. We've used the equations shown in Fig. 8 to produce a nomogram which, when used with measurements of the PCP ray arrival time multiplied by the wave speed in the matrix material, and measurements of the arrival time of the PFFP ray, can then be used to determine the inclusion size and inclusion fluid wave speed(see Fig. 9).

It's clear from this that measurements of the arrival times of the scattered pulses are all that we need for the quantitative NDE of materials, at least for the simple inclusion geometry we have considered.

Well, what about the spectra? The spectra, when we took the spectra of the A_1 amplitude alone - you remember that was the first signal returning from the inclusion - and we compared its spectrum to that we obtained for the specular reflection echo from the flat back wall of the specimen, there were pronounced differences. The spectra showed a dependence on the inclusion radius. In other words, we do detect an effect dependent on the inclusion curvature. Unfortunately, at the present time, we don't really understand what the exact relationship between curvature and its effect on the spectra is.

On the other hand, if we include all of the scattered signals, that is A_1, a_1, a_2, A_2 and A_3, in our spectrum analysis, we obtain spectra which look like those shown in Fig. 10. Figure 10(a) is the case of a 1/32" dia. alcohol inclusion in Lucite while Fig. 10(b) is the case of a 1/8" dia. inclusion. On the ordinate we have the amplitude and on the abscissa we have the frequency in megahertz. One observes a pronounced modulation in the spectra, and it depends quite critically on the size of the inclusion and what the inclusion material's wave speed are. These spectra appear similar to the spectra one obtains if one observes the resonances of a multi-degree of freedom vibrating system. I'll return to this point a little later.

We found an empirical equation relating the characteristics of the inclusion to features in the spectra. That is, the frequency intervals between successive maxima or minima are given by the quotient of c_f, which is the wave speed in the fluid divided by 2d, where d is the inclusion diameter.

We showed in a recent publication[7] that the same arrival time analysis and the spectrum analysis is applicable to the case of a solid inclusion provided that the wave speed in the solid is less than the wave speed in the fluid. We have made measurements on solid inclusions such as Lucite, glass, brass, iron and quartz in an aluminum matrix and we find that all the equations and all our ideas regarding the fluid-filled inclusions apply.

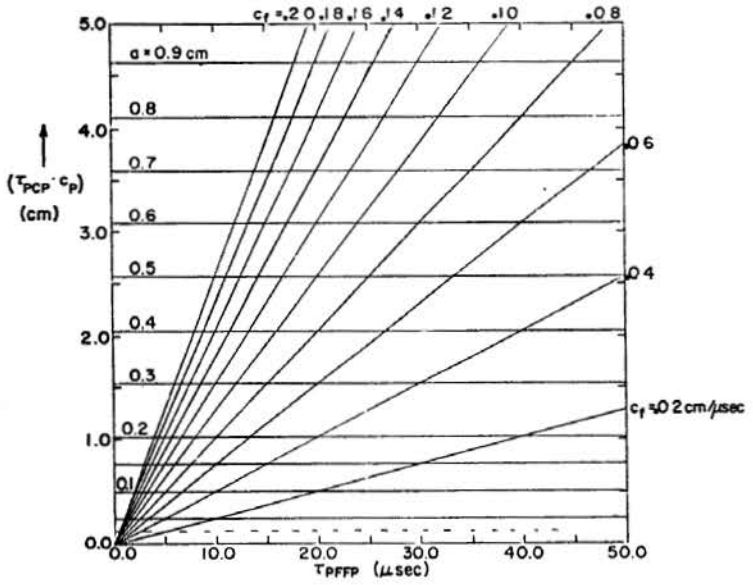

Fig. 9. Nomogram for the evaluation of the inclusion radius a and inclusion fluid wave speed c_f from τ_{PCP} and τ_{PFFP} measurements.

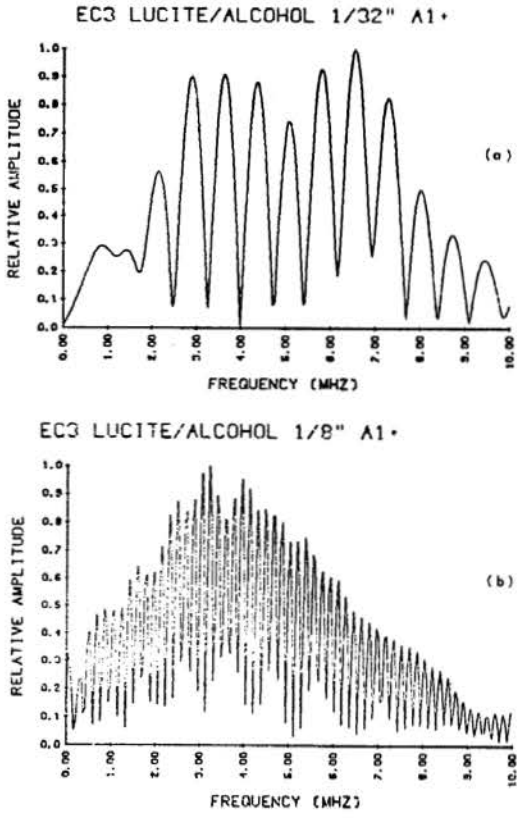

Fig. 10. Spectra of the entire scattered signal from an alcohol-filled inclusion in lucite. (a) 1/32-in. diam. (b) 1/8-in. diam.

We have recently completed the initial experiments to investigate what the orientation dependence of the scattered signals is[4]. The apparatus and specimen used are shown schematically in Fig. 11. We used three transducers: one is a transmitting transducer, which serves also as receiver in the back scattering direction, another is a receiving transducer in the forward scattering direction; and a third transducer is one which we can move around at will to be used as receiver at either 45, 90 or 135 degrees. As in the experiments described previously we display all the received signals on an oscilloscope, we photograph them, digitize them, and again perform our spectral analysis.

A typical amplitude-time record one observes is shown in Fig. 12. This is the case of a 1/32 in. dia. water-filled inclusion in an aluminum block. The bottom two signals are the overall amplitude-time curves. The intensified portions of these are displayed in the delayed sweep mode in the top two traces. The uppermost trace is the back-scattered signal. As before, it consists of amplitudes A_1, a_1, a_2, A_2, A_3 and so on. The second amplitude-time trace is that which is received with a transducer at 90 degrees with respect to the transmitting transducer. Well, it's easy to do the ray analysis, so we did it, and we show in Fig. 13 what we obtain for the 90 degree scattering situation. We again observe, essentially, four rays. The first two to arrive are analogous to those we observed in the back scattering situation. We observe again a reflected ray and then a creep ray. The next signal we observe here is a ray which does not creep along the surface of the inclusion, but rather propagates through the inclusion once. The critical incident angle θ_i^* is that particular angle which is dependent on inclusion and matrix materials and which is such that the ray propagates through the inclusion and to the receiving transducer. We have a second PFFP ray and then additional ones. In comparing the computed ray arrival times with those measured, we obtain, again, agreement which is just as good as what we obtained in the back-scattering situation.

We have derived what the arrival-time dependence of the various rays is expected to be as a function of arbitrary transmitter-receiver angle. We show the results in Fig. 14. We expect the PCFP ray not to exist for angles of θ between the transmitter and receiver which are greater than $2\theta_g$, where θ_g is $\sin^{-1} cf/_{cp}$.

Because of the angular dependence of the arrival times, we expect of course, that the frequency spectra show a similar dependence. To illustrate this, we will show the results we obtained from a 1/16 in. diameter water-filled inclusion in an aluminum block. In Figs. 15(a-d) we show the spectra obtained at various transducer-receiver angles. Only the signals from A_1 through A_2 on the amplitude-time record were included in the spectral analysis. The pronounced variations in the scattered signal's spectra at the various directions are clearly evident. Pao and Mow[8] in their theory of ultrasonic spectroscopy show how to compute the spectrum of the radial stresses associated with pulses which are scattered by an inclusion in various scattering directions. They concluded from their calculations that, in the spectra of the back-scattered signals, the <u>minima</u> of the spectra coincide with $n = 0$ and $n = 1$ for the resonance frequencies and their overtones of the inclusion. For the spectra of the forward scattered signals, they computed that the <u>peaks</u> of the spectra coincide with the frequencies of all the $n = 0$ and $n = 1$ modes. In the case

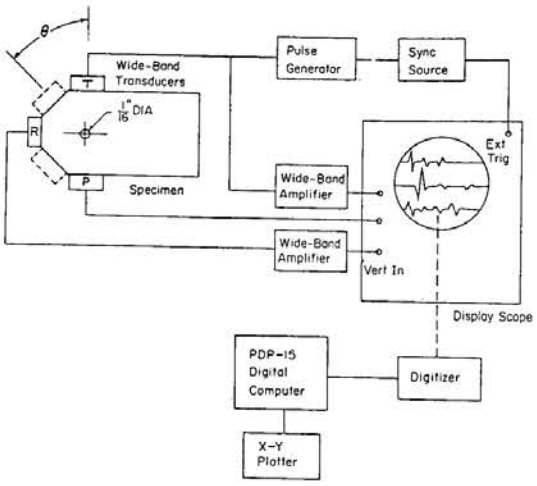

Schematic of Experimental Setup

Fig. 11. Schematic of the experimental setup for studying the orientation dependence of the scattering by a cylindrical inclusion.

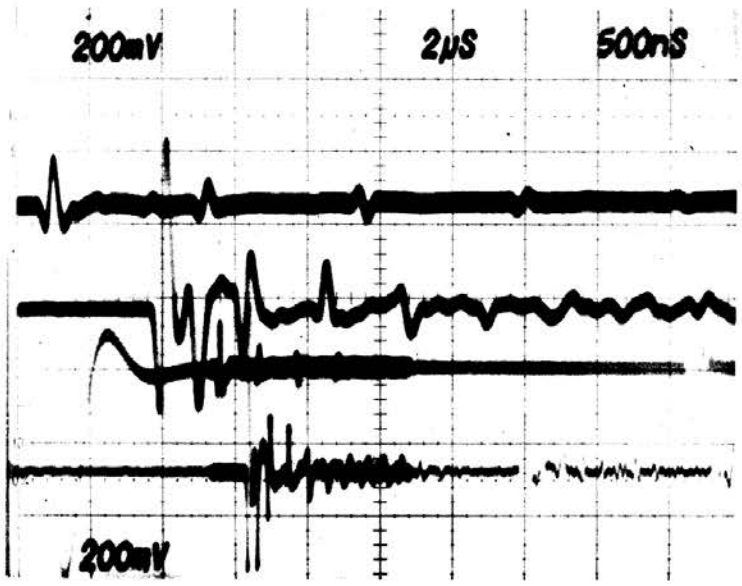

Fig. 12. Amplitude-time record of 1/32-in. diam. water-filled inclusion in aluminum. Top trace is intensified portion of back-scattered signal. Second trace is intensified portion of 90°-scattered signal.

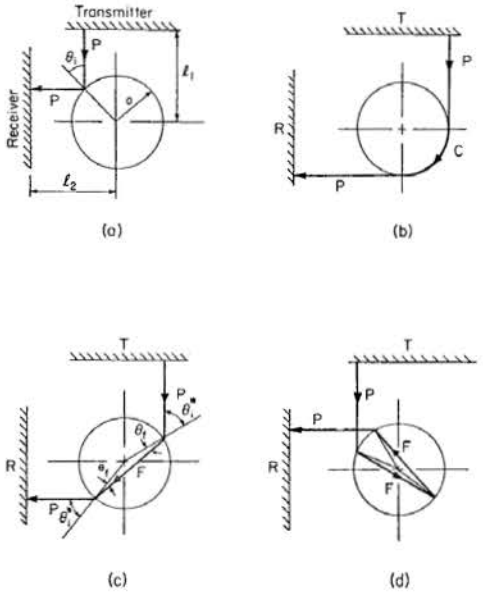

Fig. 13. Ray paths for the 90° scattering situation.

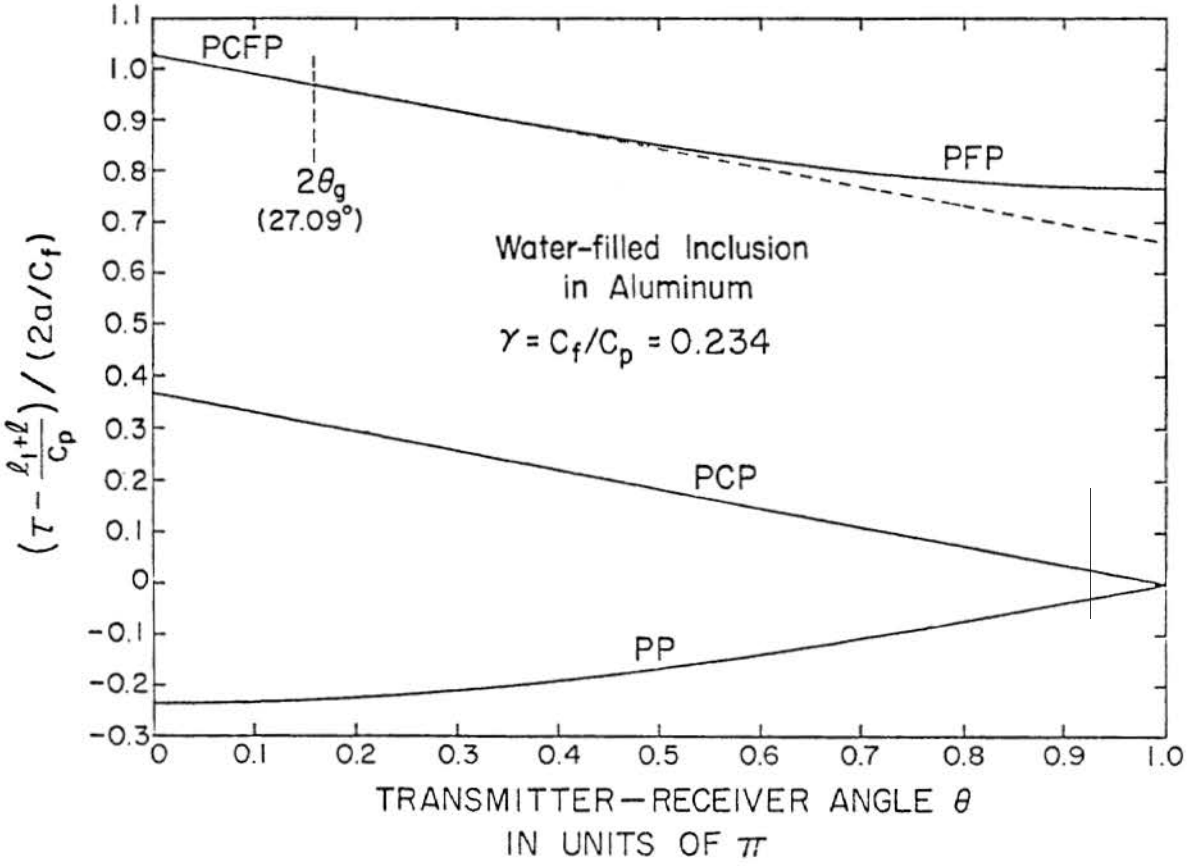

Fig. 14. Arrival-times of the various rays as a function of transmitter-receiver angle.

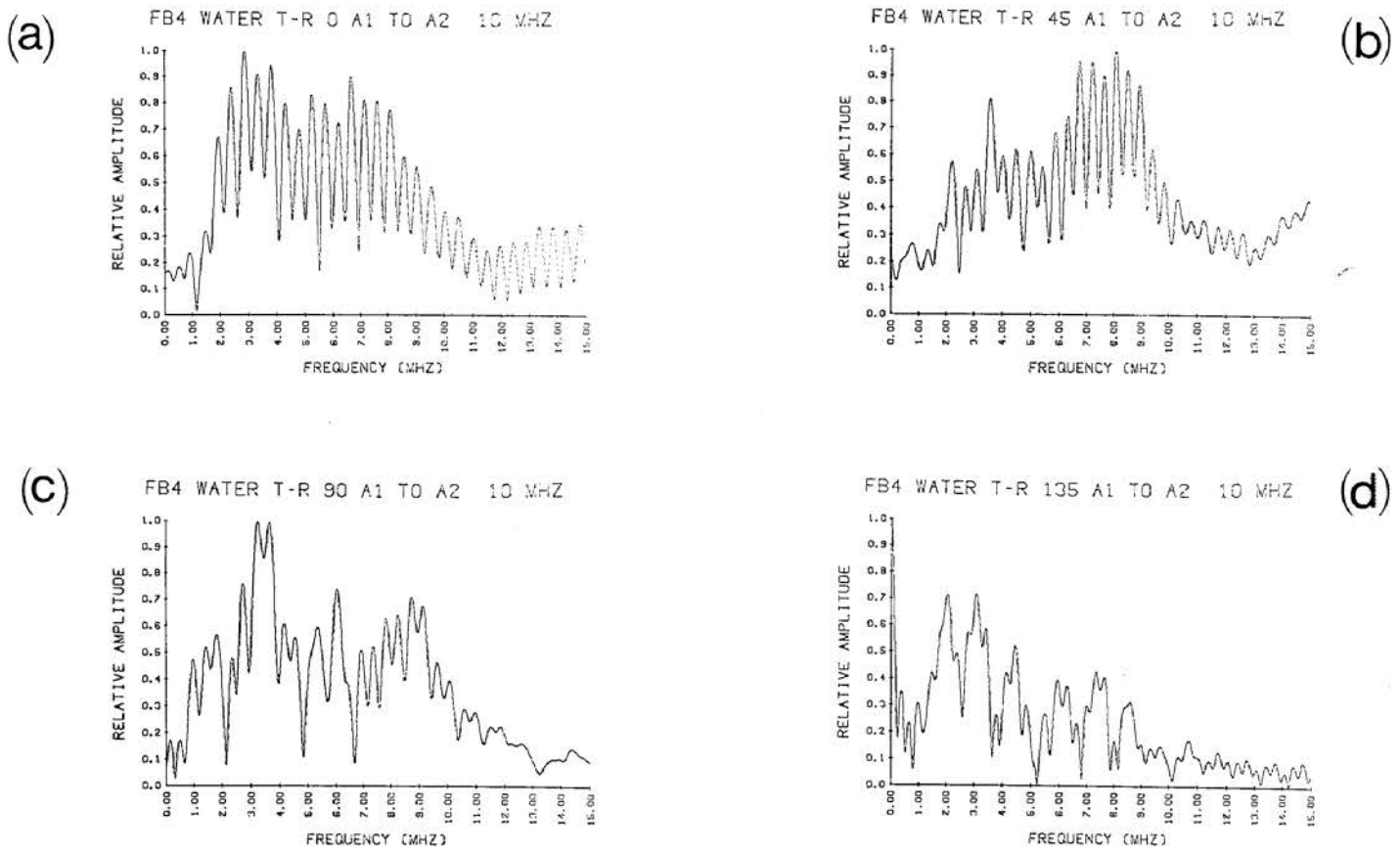

Fig. 15. Spectra of the A_1 to A_2 signal at various transmitter-receiver orientations. (a) 0° (Backscattered), (b) 45° , (c) 90° , (d) 135° .

of a 90 degree scattering situation their calculated spectra had peaks at frequencies corresponding to all the n = 0 modes.

The critical test, of course, is to make a comparison of their results with the observed spectra in the experiments. We show in Fig. 16 the results of our analysis of all the signals back-scattered from a 1/16 in. water-filled inclusion in aluminum. One sees again the pronounced modulation in the spectra. We also show in the figure lines which correpond to the frequencies of the n = 0 and n = 1 modes as computed by Pao and Mow [8] . Clearly, the minima of the observed spectra coincide with the computed minima over a wide range of frequencies.

We show in Fig. 17 the results of our analysis of the forward-scattered signals from the water-filled inclusion. Now the peaks of the spectrum coincide with the frequencies of the n = 0 and n = 1 modes. We have not yet obtained reproducible spectra for the 90 degree and the other scattering situations. These will have to be obtained first if a valid comparison between the experimentally obtained spectra and the normal mode theory of Pao and Mow is to be made.

I'm sorry that I'm out of time. I had hoped to have time to describe for you the measurements and the ray analyses we have made on two inclusions or a bi-inclusion. Let me report that the amplitude-time records become quite complicated; however, we can clearly identify numerous rays in these amplitude records. We need, however, to identify only four rays in order to completely specify the location, the separation, the radius and the wave speed of the fluid in such inclusions, and we have done that. However, we believe that this is probably the most complex scattering situation that we can easily study from such arrival-time measurements. As I stated, we require only four distinct rays for the complete specification of the parameters of the scatterer; there exist in fact, 30 or more and it becomes very difficult to sort out the particular ones which one needs to specify the properties of the bi-inclusion or the two inclusions.

Now, the inevitable conclusion that we've reached from this work is that for the scattering cases that we have considered, the arrival times are all that we need to determine all we want to know about the scatterer. We recognize, however, that there will probably be cases in which the arrival-time measurements are going to be very difficult to make, as for example, the bi-inclusion. For these kinds of situations we expect that ultrasonic pulse spectroscopy measurements to be very useful. We believe, however, that they must be interpreted in terms of the normal mode theory of the scatterer.

Thank you.

References:

1. W. Sachse, J. Acoust. Soc. Am., 56, 891-896 (1974).

2. Y. H. Pao and W. Sachse, J. Acoust. Soc. Am., 56, 1478-1486 (1974).

3. W. Sachse and C. T. Chian, Matls. Eval., 33, 81-88 (1975)

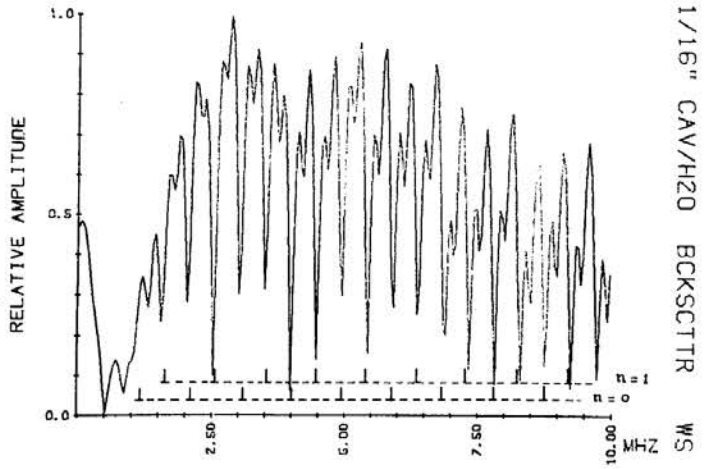

Fig. 16. Spectrum of the entire back-scattered signal from a 1/16-in. diam. water-filled inclusion in aluminum. Also shown are the inclusion's resonance frequencies of its $n = 0$ and $n = 1$ modes.

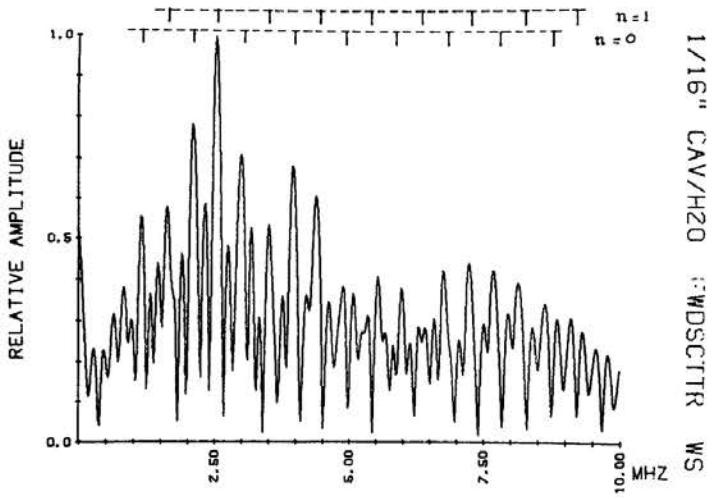

Fig. 17. Spectrum of the entire forward-scattered signal from a 1/16-in. diam. water-filled inclusion in aluminum. Also shown are the inclusion's resonance frequencies of its $n = 0$ and $n = 1$ modes.

4. F. Bifulco, Dissertation, Cornell University, Ithaca, N.Y. (Jan. 1975).

5. W. Sachse, F. Bifulco and Y. H. Pao, Materials Science Center Report #2548m Cornell University, Ithaca, N.Y. (1975). Submitted to J. Acoust. Soc. Am.

6. W. G. Neubauer, in Physical Acoustics, Vol. X, Chapt. 2, W. P. Mason and R. N. Thurston, Eds., Academic Press, New York (1973).

7. F. Bifulco and W. Sachse, Ultrasonics, 10, 113-116 (1975).

8. Y. H. Pao and C. C. Mow, Materials Science Center Report #2547, Cornell University, Ithaca, N.Y. (1975). Submitted to J. Acoust. Soc. Am.

DISCUSSION

DR. TOM WOLFRAM: We have got about two minutes for questions. In the back?

DR. JIM SEYDEL (University of Michigan): I gather you feel that this is only applicable to fluid filled cavities and not air filled?

DR. SACHSE: We have considered, of course, the air filled cavity also. For this case we find that we do, in fact, see the PP ray and the PCP ray. Then we observe some noise in our amplitude time record. We believe that if we use very high amplification and possibly signal processing techniques, we could, in fact, find the other rays which correspond to the "halo" ray and the PFFP ray.

DR. SEYDEL: What velocity did you use for the PCP ray?

DR. SACHSE: The velocity of the matrix material,

DR. SEYDEL: I though that it was a function of the radius of the inclusion.

DR. SACHSE: We didn't find that. The agreement between theory and experiment for the cases we considered, which was 1/32 inch diameter to 1/8 inch diameter cavities, is in all cases very good.

DR. HENRY BERTONI (Polytechnical Institute of New York): Your nomograms there relate to the spherical cavity?

DR. SACHSE: No, cylindrical.

DR. BERTONI: Cylindrical, I'm sorry, in your case. But if you are going to some cavity, would you comment on whether you can, for an ellipsoidal cavity or ellipsoidal cylinders, use similar results to compute the properties and the shape?

DR. SACHSE: I think that possibly you'd get some sort of average radius for these cases, provided that the scatterer doesn't have a sharp edge on it. But again, one would probably measure an average radius. In the case of the back scattering situation, the PCP ray would, of course, be related to the half-circumference of the ellipse. One would have to be aware of these things in applying our equations to other geometries.